



A model for the binding of low molecular weight inhibitors to the active site of thrombin

Mark C. Allen*, Xiao Ling Fan Cockcroft**, Markus G. Gruetter*** & John P. Priestle****
Novartis Horsham Research Centre, Wimbleshurst Road, Horsham, West Sussex RH12 4AB, U.K.

Received 20 November 1998; Accepted 1 February 1999

Key words: anti-thrombotics, conformational searching, molecular mechanics, X-ray coordinates

Summary

This paper describes the construction, validation and application of an active site model of the serine protease thrombin. Initial use was made of medium resolution X-ray crystallographic structures of thrombin complexed with low molecular weight, non-specific inhibitors to create a computationally useable active site shell of the enzyme. Molecular mechanics methods were then applied to dock known ligands into the active site region in order to derive a model that would accurately predict binding conformations. Validation of the modelling process was achieved by comparison of the predicted enzyme-bound conformations with their known, crystallographic binding conformations. The resultant model was used extensively for predictive purposes prior to obtaining confirmatory crystal data relating to a ligand possessing a novel and unexpected binding component complexed to thrombin. The data served both to confirm the accuracy of the binding site model and to provide information for the further refinement of the model.

Introduction

The central role of thrombin (EC 3.4.21.5), a serine protease, in the maintenance of hemostasis and in the blood coagulation cascade, marks it out as a relevant target for inhibition in the search for anti-thrombotic therapies [1]. This view is supported by the published activity of a number of laboratories aimed at discovering and developing novel, selective and effective thrombin inhibitors [2]. Recent attempts to improve anti-coagulant and anti-thrombotic therapies have derived either through parenteral-only treatments (e.g. hirudins [3] and hirulogs [4]), or through the enhancement of selectivity and tolerability of potentially orally

available low molecular weight compounds (e.g. argatroban [5]).

We, like others [6] have embarked on a course of study to address the latter requirement by structure-based design methodology and have directed our approach to non-transition state, reversible inhibitors rather than those forming covalent links with the enzyme. The latter approach is typified by PPACK (D-phenylalanyl-L-prolyl-L-arginine chloromethylketone, **1**), and is relevant here only in that it provided the first solved X-ray crystal structure of a thrombin–ligand complex [7] (1.9 Å resolution). Other, more relevant structures have included Banner's [8] series of thrombin complexes with reversible low molecular weight inhibitors, comprising benzamidine (3.0 Å resolution), NAPAP (N^α–[(2-naphthylsulfonyl)glycyl]-4-amidinophenylalanylpiperidine, **2**, 3.0 Å resolution), and MD805 ((2*R*,4*R*)-4-methyl-1[N^α–[(3-methyl-1,2,3, 4-tetrahydro-8-quinolyl)sulfonyl]-L-arginyl]-2-piperidinecarboxylic acid, **3**, 3.0 Å resolution), which served as the lead compound for this study.

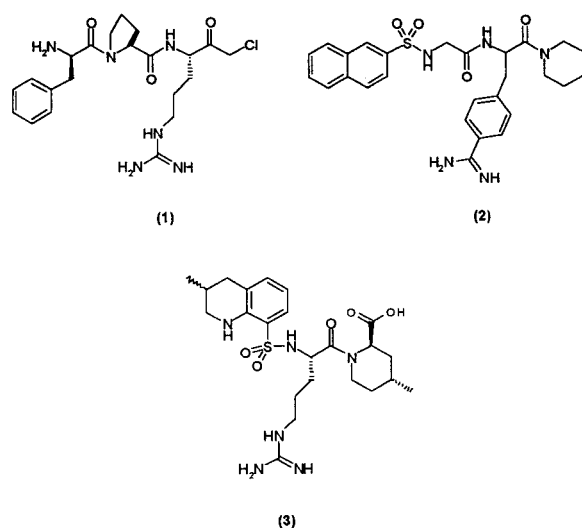
*To whom correspondence should be addressed. Present address: Tripos Receptor Research Ltd., Tamar Laboratories, Bude-Stratton Business Park, Bude, Cornwall EX23 8LY, U.K.

**Present address: Xenova Ltd., 240 Bath Road, Slough SL1 4EF, U.K.

***Present address: Department of Biochemistry, University of Zürich, Winterthurerstrasse 190, CH-8057 Zürich, Switzerland.

****Present address: Novartis Pharma AG, CH-4002 Basel, Switzerland.

We report here the identification and construction of an atomistically defined portion of thrombin incorporating the active site region based on crystallographic data, and its modification to a chemically accurate and computationally useful model. We report also the docking to this model of a variety of ligands of known (from crystal data) and unknown binding conformation by molecular mechanics methods and the evolution of a validated method with a defined set of parameters that allows the prediction of binding conformations of novel ligands.



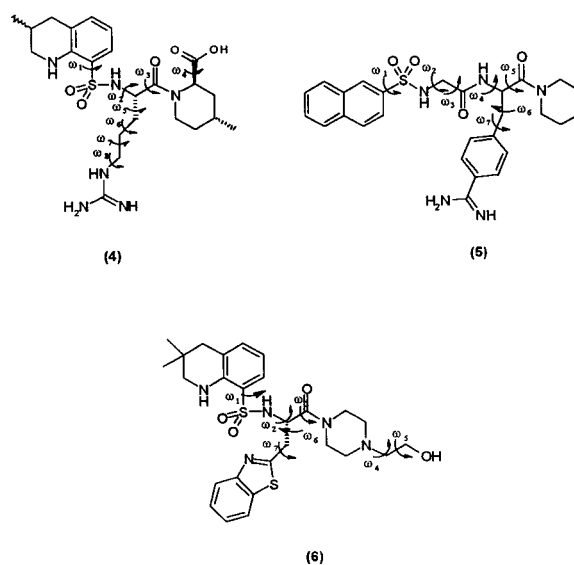
Materials and methods

Structural visualisation and editing, molecular mechanics calculations, energy minimisations and conformational searches were performed with the Macro-Model 3.1/BATCHMIN 3.1 software package [9], using the AMBER force field [10]. Docking was achieved by the application of a modified Monte Carlo (MC) Search–Energy Minimization (EM) protocol, first described by Guida [11], where low energy binding conformations of a ligand are determined by repeated energy minimisations of a series of Monte Carlo search generated conformations.

Construction of the initial active site shell

The working active site shell was initially created from the X-ray crystal structure of thrombin complexed to MD805 [8] (Brookhaven Protein Data Bank ID Code: 1DWC). All active site residues within 5 Å of the ligand were included in the shell. Those residues that were only partially included by the 5 Å cut-off

had their sequences completed, and all the resulting strands making up the shell were terminated either as N-acetyl- (amino termini) or N-methylcarboxamide- (carboxy termini) derivatives. In addition, proline residues (60B and 60C) [12] in the loop region were included. The ϵ -amino function of lysine 60F was protonated, histidine 57 was singly protonated (on the π -nitrogen of the imidazole ring), and the ω -carboxy groups of aspartic acids 189 and 194 and glutamic acids 192 and 217 were represented in anionic form. The completed shell was minimized using the Polak-Ribiere conjugate gradient algorithm (PRCG) with a parabolic restraining force constant of 500 kJ/Å² with respect to X-ray positions on all but two methyls at distal positions of the shell.



Knowledge of the ability of an enzyme to flex, or slightly alter its conformation to accommodate a binding ligand, is crucial to the process of predicting or modeling new inhibitors. Access [8] to the crystal structures of thrombin complexed separately with four low molecular weight ligands enabled us to directly compare the relative positions of their active site residues, with an accuracy limited by the resolution of the solved structures (3.0 Å). Table 1 lists those residues, and describes their positions relative to the thrombin–MD805 complex. Deviation from the thrombin–MD 805 position is defined by the distance displaced for each active site residue. The distances quoted are for the α -carbon and the residue atom that is displaced the most, and those that exceed 0.5 Å are emboldened.

Table 1. Comparison of active site residue positions in thrombin–ligand complexes in relation to their position in the thrombin–MD 805 complex

Position [11]	Residue	MD805–PPACK		MD805–NAPAP		MD805–benzamide	
		C $^{\alpha}$ position (Å)	Side-chain position (Å)	C $^{\alpha}$ position (Å)	Side-chain position (Å)	C $^{\alpha}$ position (Å)	Side-chain position (Å)
57	Histidine	0.31	0.82	0.14	0.24	0.22	0.25
60A	Tyrosine	0.23	0.31	0.42	0.67	0.32	0.44
60D	Tryptophan	1.30	1.94	0.32	0.92	0.36	0.98
60F	Lysine	0.37	1.33	0.21	0.23	0.10	0.09
192	Glutamic acid	0.57	4.08	0.22	0.21	0.20	0.20
195	Serine	0.27	0.92	0.06	0.17	0.11	0.08
216	Glycine	0.55	0.55	0.51	0.51	0.29	0.29

Distances that exceed 0.5 Å are in bold.

Table 1 shows the expected conservation of active site residue position typical of the serine protease family, with the greatest differences apparent in the comparison of the thrombin–PPACK complex, reflecting the irreversible, covalent nature of the PPACK ligand binding mode. The findings also illustrate the mobility of the residues in the ‘60-loop’ region, and in particular the tryptophan and tyrosine residues. On the basis of these observations we were able to incorporate a level of flexibility within the model, by removing or reducing the energy constraints on the atoms of the moveable residues of the active site. Consequently, during docking, or sub-structure minimisation procedures within the active site, all the atoms of the ligand and the side-chain of serine 195 were allowed complete freedom, atoms of residues tyrosine 60A, tryptophan 60D, lysine 60F and glycine 216 were constrained with a parabolic restraining force constant of 10 kJ/Å², whilst all other residues of the active site shell were constrained with a parabolic restraining force constant of 500 kJ/Å². Allowing serine 195 freedom of movement would enable the hydroxyl function to re-orient to enable the maximum degree of hydrogen bonding either with the ligand or with solvent molecules. We were able subsequently to refine and simplify this protocol: allowing the ligand and serine 195 to minimise freely; residues tyrosine 60A, tryptophan 60D, lysine 60F, glutamic acid 192 and glycine 216 to be held with a parabolic restraining force constant of 10 kJ/Å²; and the remaining amino acid residues held with a parabolic restraining force constant of 500 kJ/Å².

Computational methods and conditions

The application of the AMBER force-field in MacroModel assumes addition of explicit hydrogens to heteroatoms alone. However, we have found that the addition of explicit hydrogens to aryl moieties better models the electrostatic interactions [11]. Parameterization of the oxygens of the sulfonamide bond as O-single bonds rather than O-double bonds was also found to improve the fit. A distance dependant dielectric constant was employed since it had been previously noted that non-distance dependence for the dielectric constant had caused an overestimation of the total electrostatic forces [11]. All electrostatic charges were further attenuated by a factor of 4 since initial energy minimisation studies had shown this to provide an optimal fit with the X-ray structure. For reasons of uncertainty relating to the position of solvent molecules, and our limited computational processing power, solvent molecules were initially excluded from the active site shell.

Inhibitors whose binding conformations were unknown were initially placed in the active site with the aid of molecular graphics in a conformation approximating that which we believed to be the active conformation. As our confidence in the model grew, we were able to place inhibitors in the active site in a completely arbitrary fashion including some very high energy conformations. Conformational searches used the method of Chang, Guida and Still [13] where the structure for each MC step was selected from previously saved low energy structures with preference given to those used fewest times in previous steps, and then energy minimised. New structures were retained if they did not exactly duplicate previous structures and if they were within 25 kJ/mol of the current min-

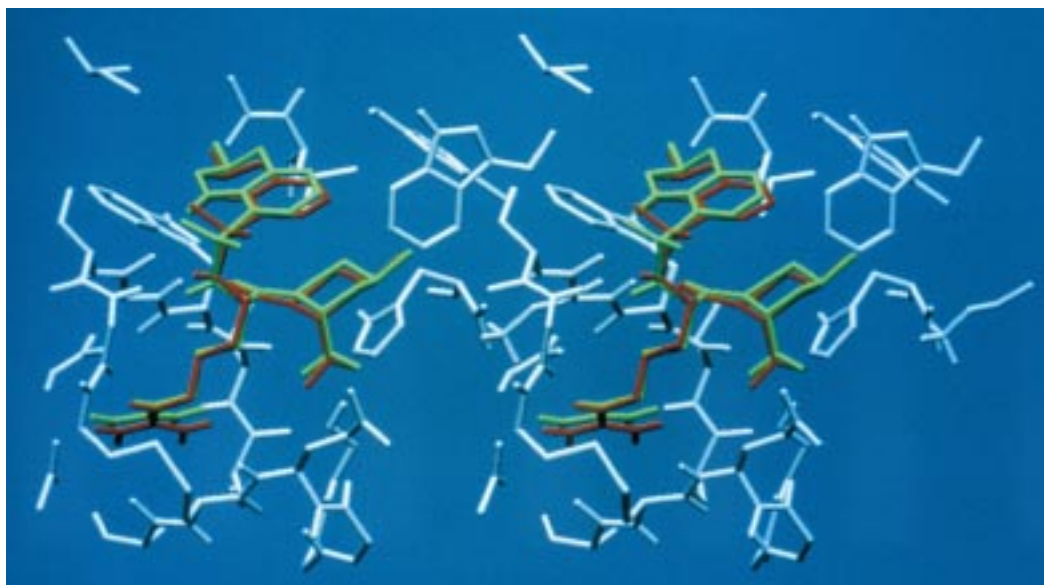


Figure 1. Model for the binding of MD 805 at the active site of thrombin. A global minimum energy conformation of MD 805 (red) is shown overlaid on the experimentally derived conformation (green) in a portion of the crystallographically determined active site region of thrombin (grey).

imum energy conformation. During each MC step, between two and four randomly selected torsion angles were allowed to vary simultaneously. Typically 2000 MC steps were employed for each conformational search. The Polak–Ribiere conjugate gradient minimiser algorithm was used for all energy minimisations (typically 300 iterations or until the energy gradient rms fell below 0.10 kJ/Å).

All computations were performed on a Silicon Graphics 4D/35 (R4000 processor) workstation.

Results and discussion

Structure 4 illustrates those torsion angles for the inhibitor MD805 utilised in an MC/EM conformational search in the original active site model described above.

An arbitrary starting conformation was used and 2000 MC/EM steps yielded 27 low energy conformations within 25 kJ/mol of the minimum energy conformation. A second search starting from a different conformation gave an identical minimum energy conformation following 2000 MC/EM steps, though a largely different set of low energy conformations within the 25 kJ/mol energy window. Conformations within the sets exhibited significant binding differences, where the expected interactions of P1, P2 or P3

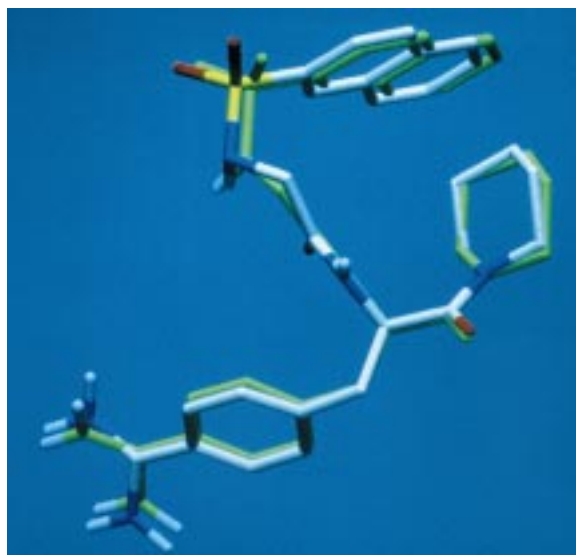


Figure 2. Comparison of the binding conformations of NAPAP. The experimentally determined conformation (green) of NAPAP is shown superimposed on the global minimum energy conformation of NAPAP (atom colors) derived from the initial model.

binding portions were not always observed. Our ability to find convergent minima using only 2000 steps probably reflects the constrained nature of the binding site and the choice of relevant minimiser algorithm.

A comparison of the 'crystal' and 'modeled global minimum energy' conformations based on their tor-

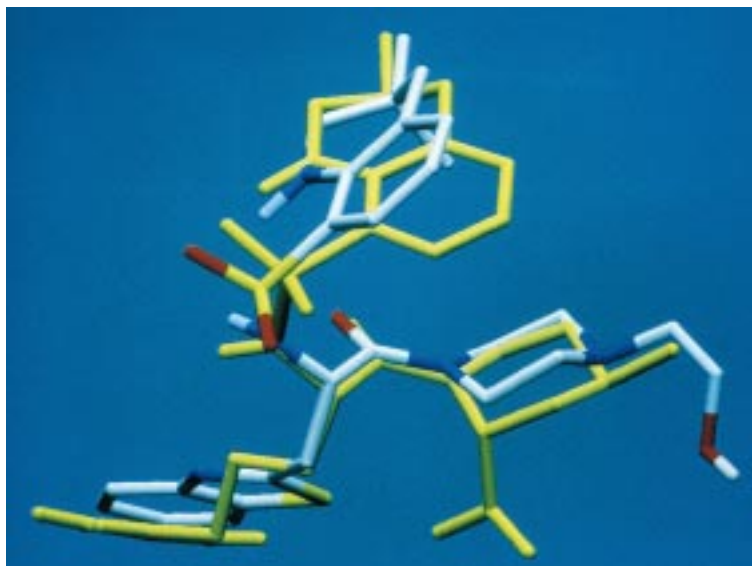


Figure 3. Comparison of the binding conformations of MD 805 and CGH 771. The crystallographically determined binding conformation of MD 805 (yellow) is shown overlayed on the global minimum energy conformation of CGH 771 (atom colors) determined from the initial model.

Table 2. Comparison of experimental and modelled torsion angles for the thrombin–MD 805 complex

Torsion angle ^a	X-ray conformation	Global minimum energy conformation
ω_1	−90.4	−99.5
ω_2	−85.8	−83.2
ω_3	149.6	151.5
ω_4	166.2	93.5
ω_5	35.9	58.9
ω_6	170.5	179.1
ω_7	179.6	177.5
ω_8	108.7	89.9

^aTorsion angles as depicted in structure 4.

Table 3. Comparison of experimental and modelled torsion angles for the thrombin–NAPAP complex

Torsion angle ^a	X-ray conformation	Global minimum energy conformation
ω_1	−109.5	−104.9
ω_2	−127.5	−128.2
ω_3	−170.8	−149.5
ω_4	121.6	116.2
ω_5	−81.2	−84.3
ω_6	70.2	71.1
ω_7	−88.9	−88.3

^aTorsion angles as depicted in structure 5.

sion angles is given in Table 2. Figure 1 shows the two structures superimposed on the thrombin active site region. The root-mean-square deviation (rmsd) between all atoms (except hydrogens) for the two conformers was 0.39 Å.

The most significant deviation from the experimental structure occurred for the piperidine carboxyl torsion (ω_4). This observation was not unexpected since the carboxylate anion would be able to interact with solvent molecules that were absent from our initial model. This assumption was validated by subsequent work on the refined active site model.

In order to establish the applicability of this model to non-arginine containing ligands we docked NAPAP into the active site model in an exactly analogous manner to that described above, yielding 43 low energy conformers. A comparison of the torsion angles of the experimental and global minimum energy conformation is given in Table 3. Figure 2 shows an overlay of the two structures. The rmsd between all atoms (except hydrogens) for the two conformers was 0.28 Å, again providing an indication of the accuracy of our model in predicting the binding conformation. The improved rmsd value for NAPAP over MD 805 probably reflects the fewer flexible torsions and the presence of fewer potential hydrogen-bonding functionalities.

The ability to accurately predict the binding conformations of MD 805 and NAPAP gave confidence that we could use our model to evaluate potential inhibitors prior to synthesis and so provide a modeling filter to synthetic candidate compounds. We subsequently and successfully applied our model to the design and assessment of in-house inhibitor candidates for a period of six months, deriving valuable structure–activity relationships (which will be discussed in full in a subsequent paper). Within the series of modeled compounds we synthesised the non-arginine containing thrombin inhibitor, CGH 771 (3,3-dimethyl-1,2,3,4-tetrahydro-quinoline-8-sulfonic acid-{1(S)-benzothiazol-2-ylmethyl-2-[4-(2-hydroxy-ethyl)-piperazin-1-yl]-2-oxo-ethyl}-amide, **6**) shown subsequently to possess good activity. CGH 771 possessed structural similarities to MD 805 in the proposed P2 [14] and P3 binding portions of the molecule, though differed markedly in what we believed to be the P1 binding portion, where the ‘usual’ basic side chain was replaced by the benzthiazole moiety. The replacement of the basic side chain resulted in inhibitors possessing three neutral, aromatic or alicyclic portions. We could not be certain that the central amino acid, now containing the benzthiazole

side chain, would continue to bind in the P1 binding pocket; indeed, accepted wisdom indicated that only strongly basic residues such as guanidines and amidines were effective substrates for the P1 binding pocket of thrombin. Confirmation, or otherwise, of the binding of the benzthiazole moiety in the P1 binding pocket of thrombin was therefore crucial to the further design of analogs and our structure–activity relationship studies. Application of the MC/EM methodology as described provided 48 low energy conformers within 25 kJ/mol of the global minimum energy conformation. Figure 3 represents a view of the global minimum energy conformation of CGH 771 superimposed on the binding conformation of MD 805. The result obtained confirmed our assumption that the benzthiazolylalanine moiety (Bta) of CGH 771 bound in the P1 binding pocket, in fact the 40 lowest energy conformations (all within 20 kJ/mol of the global minimum energy conformation) showed the Bta moiety to bind in this way.

The ability of Bta to mimic arginine is not obvious. The absence of any conventional active site director such as guanidine or amidine is clear, as is the lack of any ion-based interaction of the Bta side chain with the ω -carboxyl function of Asp 189 at the base of the P1 binding pocket. However, the lipophilic interaction of the propyl component of the arginine side chain with the residues that make up the wall of the P1 binding pocket (Ala 190, Cys 191, Gly 216, Cys 220 and Trp 237) would appear to be most effectively mimicked by the aromaticity of Bta. In addition, the lipophilic interactions between the ligand and the residues that define the P3 (Trp 215, Ile 174, Leu 99) and P2 binding pockets (Trp 60D, Tyr 60A and His 57) appear significant. This conclusion is supported by recently published work [15] where non-basic residues are found to bind in a similar manner. Whether the P1 pocket binding provides a sufficient contribution to binding affinity in the absence of any strong P2 and particularly P3 lipophilic binding pocket interactions is not clear, though the ability of Bta to mimic arginine in other serine protease enzymes should provide some indication. A comparison of amino acid residues that comprise the wall of the P1 binding pocket of a number of serine proteases reveals significant differences at position 190. In thrombin, as in chymotrypsin, this position is occupied by alanine, whereas in those proteases that cleave after arginine, namely trypsin, plasmin, kallikrein, h-factor VIIa and factor IXa position 190 is occupied either by serine or threonine. Thrombin might therefore be consid-

ered to possess a P1 binding pocket representing a hybrid of chymotrypsin and trypsin, with the capability of accommodating both lipophilic (due to Ala 190 rather than Ser/Thr 190) and basic substrate sidechains (Asp 189 rather than Ser 189 in chymotrypsin). Such an argument would suggest that Bta would not be a universal alternative replacement to arginine.

Resolution of a crystal structure of thrombin complexed to CGH 771 by Gruetter et al. [16] subsequently showed our model to have predicted the binding conformation with a high level of accuracy.

The rmsd between all atoms (except hydrogens) of the modeled and experimental CGH 771 conformers was 1.30 Å, and differed most significantly in the orientation of the benzthiazole side chain, as reflected by torsion ω_7 and indicated in Table 4. In all other respects the conformation matched that of the experimental crystal structure and provided further support to the accuracy of the model.

Resolution of the crystal structure of thrombin complexed to CGH 771 (to 2.0 Å resolution) provided additional information relating to the flexibility of the active site residues and real data regarding the number and positions of bound solvent molecules. We were able to identify six such water molecules within a 5 Å distance of the bound ligand in the active site region of the crystal structure, as indicated in Table 5.

On the basis of this additional information we were able to refine our active site model (Figure 5) in the following manner:

- We extended the active site shell region to include all residues within 7 Å of the bound ligand.
- We incorporated all solvent molecules within 3.0 Å of the bound ligand and all those that were close enough to form hydrogen bonds (as predicted by MacroModel) either with the ligand or the active site residues – solvent numbers 28, 48 and 106.
- During the sub-structure minimisation process the ligand and all three solvent molecules were allowed complete freedom of movement.
- Residues histidine 57, tyrosine 60A, tryptophan 60D, lysine 60F, glutamic acid 192, serine 195 and glycine 216 were constrained with a parabolic restraining force constant of 10 kJ/Å² with respect to the X-ray positions.
- All other residues were subject to a parabolic restraining force constant of 500 kJ/Å² with respect to the X-ray positions.
- All other parameters of the original model were retained.

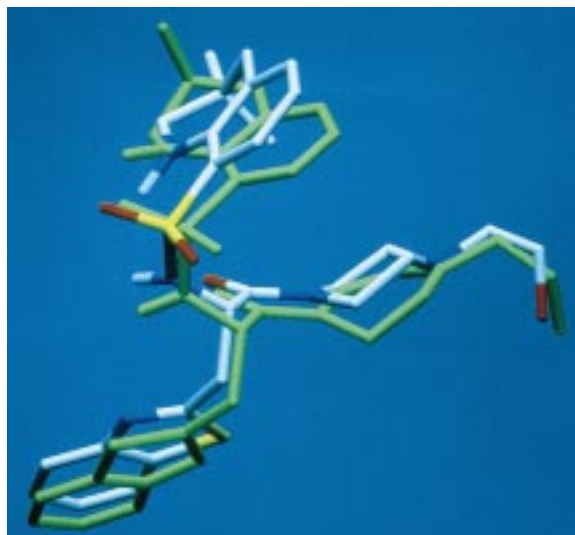


Figure 4. Comparison of the binding conformations of CGH 771. The crystallographically determined binding conformation of CGH 771 (green) is shown superimposed on the global minimum energy conformation of CGH 771 (atom colors) as determined by the initial active site model.

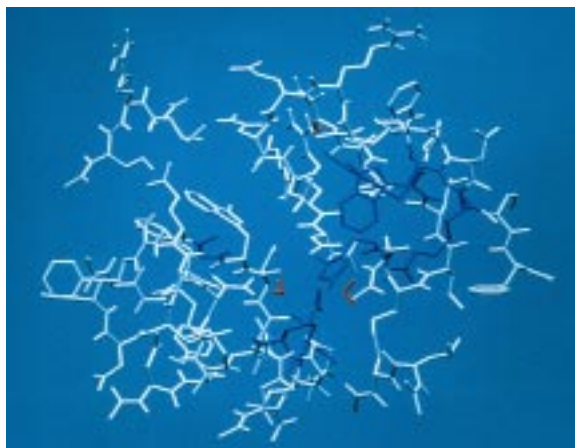


Figure 5. Representation of the refined thrombin active site model. The amino acid residues that comprise the 7 Å region around the active site of thrombin are shown, and are composed of those residues (grey) that are fixed with a 500 kJ/Å² energy constraint during the modeling process, and those held less rigidly (blue) with a 10 kJ/Å² energy constraint. Water molecules are shown in red.

Reapplication of the refined model to our existing structures – MD 805, NAPAP and CGH 771 – showed improved predictions for MD 805 and CGH 771, and prediction of the same conformation for NAPAP, as indicated in Tables 6, 7 and 8. An improved fit was observed for MD 805 (Table 6), with the greatest improvement in the P2 binding site (rmsd reduction of 0.18 Å), probably reflecting the better handling of

Table 4. Comparison of experimental and modelled torsion angles for the thrombin–CGH 771 complex

Torsion angle ^a	X-ray conformation	Global minimum energy conformation
ω_1	−107.8	−131.9
ω_2	−99.6	−117.6
ω_3	154.7	153.5
ω_4	49.7	63.0
ω_5	66.2	43.3
ω_6	58.0	76.0
ω_7	95.0	−94.3

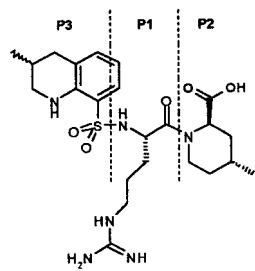
^aTorsion angles as depicted in structure 6.

Table 5. Positions and hydrogen bonding of active site solvent molecules

Solvent number	Hydrogen-bond to ligand	Nearest part of ligand	Distance (Å)
12	No	C4 of benzthiazole ring	4.99
28	Yes, to O of ethanoyl piperazine	O of ethanoyl piperazine	2.09
40	No	C5 of benzthiazole ring	3.18
48	No ^a	C4 of dimethyltetrahydroquinoline ring	4.59
106	Yes, to N of benzthiazole	N of benzthiazole ring	2.10
144	No	O of sulfonamide	4.37

^aHydrogen bond formed with phenolic oxygen of Tyr 60 (1.92 Å distant).

Table 6. Comparison of the rms deviations (Å) between experimental and modelled conformations of MD 805 complexed to thrombin



Conformation ^a	All atoms ^b	P1	P2	P3
Model 1 ^c	0.38	0.17	0.46	0.15
Model 2 ^d	0.37	0.16	0.28	0.20

^aGlobal minimum energy conformation.

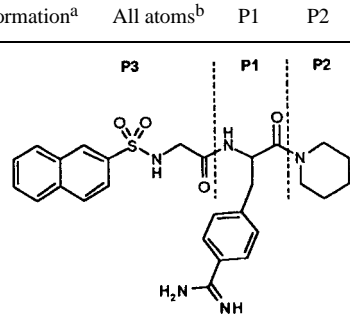
^bExcluding hydrogen atoms.

^cInitial model, no solvent molecules present.

^dRefined model, solvent molecules included.

the piperidine carboxyl now hydrogen bonding with solvent molecule 106. The identical global minimum energy conformation was obtained from both models in the case of NAPAP binding to thrombin (Table 7).

Table 7. Comparison of the rms deviations (Å) between experimental and modelled conformations of NAPAP complexed to thrombin



Conformation ^a	All atoms ^b	P1	P2	P3
Model 1 ^c	0.28	0.22	0.03	0.19
Model 2 ^d	0.28	0.22	0.03	0.19

^aGlobal minimum energy conformation.

^bExcluding hydrogen atoms.

^cInitial model, no solvent molecules present.

^dRefined model, solvent molecules included.

An overall improvement in rmsd of 0.92 Å between the two models was found for CGH 771 binding, based predominantly on the correctly predicted orientation of the benzthiazolyl ring system in the

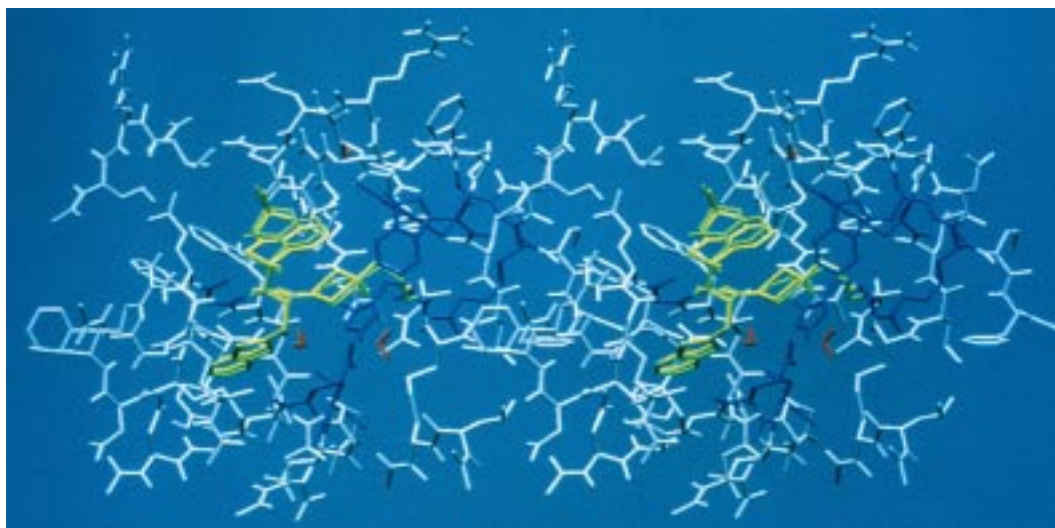
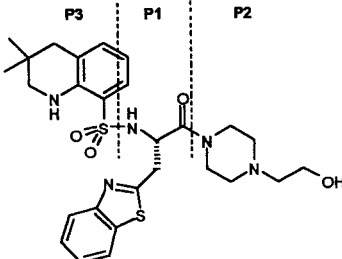


Figure 6. Comparison of the binding of CGH 771 in the refined active site model of thrombin. The experimentally determined binding conformation of CGH 771 (green) is shown superimposed on the global minimum energy conformation (yellow) as determined by the refined active site model. Also shown are the positions of the three solvent molecules (red).

Table 8. Comparison of the rms deviations (\AA) between experimental and modelled conformations of CGH 771 complexed to thrombin

Conformation ^a						
	All atoms ^b	P1	P2	P3	P1-P2	P1-P3
Model 1 ^c	1.30	1.62	0.26	0.35	1.47	1.27
Model 2 ^d	0.38	0.15	0.20	0.19	0.30	0.19

^aGlobal minimum energy conformation.

^bExcluding hydrogen atoms.

^cInitial model, no solvent molecules present.

^dRefined model, solvent molecules included.

P1 binding pocket (rmsd reduction of 1.47 \AA), see Figure 6. This again results from the more accurate treatment of the ligand as a direct consequence of including solvent, and in particular the influence of Solvent 106 in hydrogen bonding with the benzthiazolyl nitrogen and ‘fixing’ the side chain in the actual binding conformation. The representations of the P2 and P3 binding site portions of CGH 771 were also improved in the latest model, with rmsd reductions of 0.06 \AA and 0.16 \AA , respectively.

Conclusions

The study was initially undertaken to establish the feasibility of providing a modeling screen or filter for proposed synthetic candidate thrombin–inhibitor ligands. The availability of medium resolution crystal structures of thrombin complexed to our lead structure and chemically similar structures enabled us to create a provisional active site model. Using molecular mechanics methodologies we were able to dock

these ligands into the model and so assess and refine the model. Further optimisation of the modeling parameters with the subsequent good match (less than 0.5 Å rmsd) of predicted and experimental structures gave confidence that such a modeling filter for synthetic candidates was both possible and beneficial in providing significant input to the design process. The relative simplicity of the docking process allowed us typically to perform one MC/EM procedure and up to six individual EM procedures per week, given the modest processing power available to us.

The model has proven to be successful both as a filter for the selection of candidates for synthesis and as a generator of design ideas and has been used for these purposes, in varying degrees of refinement, throughout the lifetime of the project. The subsequent in house determination of the crystal structure of a novel, benzthiazole containing thrombin inhibitor further confirmed the accuracy of our model in predicting binding conformations, and allowed us to rationalise the hitherto unexpected binding of a non-basic, non-arginine containing inhibitor. The new structure also provided information that allowed us to refine our model and further improve its predictive capabilities. We have thus been able to create and provide a valuable and practical design tool that has served to improve the efficiency of the drug discovery process.

Acknowledgements

We are indebted to Dr Mark Talbot as the Thrombin Inhibitor Project Team Leader for providing the environment that allowed this work to flourish.

References

1. a. Fenton II, J.W., *Ann. N.Y. Acad. Sci.*, 485 (1986) 5.
b. Fenton II, J.W., Ofosu, F.A., Moon, D.G. and Maraganore, J.M., *Blood Coag. Fibrinol.*, 2 (1991) 69.
c. Berliner, L.T. (Ed.) *Thrombin Structure and Function*, Plenum Press, New York, NY, 1992.
d. Tapparelli, C., Metternich, R., Ehrhardt, C. and Cook, N.S., *Trends Pharmacol. Sci.*, 14 (1993) 366.
2. a. Semple, J., Minami, N.K., Tamura, S.Y., Brunck, T.K., Nutt, R.F. and Ripka, W.C., *Bioorg. Med. Chem. Lett.*, 7 (1997) 2421.
b. Tucker, T.J., Lumma, W.C., Mulichak, A.M., Chen, Z., Naylor-Olsen, A.M., Lewis, S.D., Lucas, R., Freidinger, R.M. and Kuo, L.C., *J. Med. Chem.*, 40 (1997) 830.
c. Dominguez, C., Carini, D.J., Weber, P.C., Knabb, R.M., Alexander, R.S., Kettner, C.A. and Wexler, R.R., *Bioorg. Med. Chem. Lett.*, 7 (1997) 79.
d. Wiley, M.R., Chirgadze, N.Y., Clawson, D.K., Craft, T.J., Gifford-Moore, D.S., Jones, N.D., Olkowski, J.L., Weir, L.C. and Smith, G.F., *Bioorg. Med. Chem. Lett.*, 6 (1996) 2387.
3. e. Costanzo, M.J., Maryanoff, B.E., Hecker, L.R., Schott, M.R., Yabut, S.C., Zhang, H.-C., Andreade-Gordan, P., Kauffman, J.A., Lewis, J.M., Krishnan, R. and Tulinsky, A., *J. Med. Chem.*, 39 (1996) 3039.
3. Topol, E.J., Fuster, V., Harrington, R.A., Califf, R.M., Kleiman, N.S., Kereiakes, D.J., Cohen, M., Chapekis, A., Gold, H.K., Tannenbaum, M.A., Rao, A.K., Debowey, D., Schwarz, D., Henis, M. and Cheseboro, J., *Circulation*, 89 (1994) 1557.
4. Lidon, R.M., Theroux, P., Juneau, M., Adelman, B. and Maraganore, J., *Circulation*, 88 (1993) 1495.
5. Kikumoto, R., Tamao, Y., Tezuka, T., Tonomura, S., Hara, H., Ninomiya, K., Hijikata, A. and Okamoto, S., *Biochemistry*, 23 (1984) 85.
6. a. Sanderson, P.E.J., Dyer, D.L., Naylor-Olsen, A.M., Vacca, J.P., Gardell, S.J., Dale Lewis, S., Lucas Jr., B.J., Lyle, E.A., Lynch Jr., J.J. and Mulichak, A.M., *Bioorg. Med. Chem. Lett.*, 7 (1997) 1497.
b. Tamura, S.Y., Goldman, E.A., Brunck, T.K., Ripka, W.C. and Semple, J.E., *Bioorg. Med. Chem. Lett.*, 7 (1997) 331.
c. Jiang, H., Chen, K., Tang, Y., Chen, J., Wang, Q. and Ji, R., *J. Med. Chem.*, 40 (1997) 3085.
d. Jiang, H., Chen, K., Tang, Y., Chen, J., Li, Q., Wang, Q. and Ji, R., *Acta Pharm. Sinica*, 18 (1997) 36.
e. Bertrand, J.A., Oleksyszyn, J., Kam, C., Boduszek, B., Presnell, S., Plaskon, R.R., Suddath, F.L., Powers, J.C. and Williams, L.D., *Biochemistry*, 35 (1996) 3147.
7. Bode, W., Mayr, I., Baumann, U., Uber, R., Stone, S.R. and Hofsteenge, J., *EMBO J.*, 8 (1989) 3467.
8. Banner, D.W. and Hadvary, P., *J. Biol. Chem.*, 266 (1991) 20085.
9. Mohamadi, F., Richards, N.G.J., Guida, W.C., Liskamp, R., Lipton, M., Caulfield, C., Chang, T., Hendrickson, T. and Still, W.C., *J. Comput. Chem.*, 11 (1990) 440.
10. Weiner, S.J., Kollman, P.A., Nguyen, D.T. and Case, D.A., *J. Comput. Chem.*, 7 (1986) 230.
11. Guida, W.C., Bohacek, R.S. and Erion, M.D., *J. Comput. Chem.*, 13 (1992) 214.
12. The numbering of the thrombin residues is based on Bode et al.'s protocol for chymotrypsin [7].
13. Chang, G., Guida, W.C. and Still, W.C., *J. Am. Chem. Soc.*, 111 (1989) 4379.
14. P1, P2, P3 etc., define substrate residues amino-terminal to the scissile peptide bond according to Schechter, I. and Berger, A., *Biochem. Biophys. Res. Commun.*, 27 (1967) 157.
15. a. Tucker, T.J., Brady, S.F., Lumma, W.C., Dale Lewis, S., Gardell, S.J., Naylor-Olsen, A.M., Yan, Y., Sisko, J.T., Stauffer, K.J., Lucas, B.J., Lynch, J.J., Cook, J.J., Stranieri, M.T., Holahan, M.A., Lyle, E.A., Baskin, E.P., Chen, I., Dancheck, K.B., Krueger, J.A., Cooper, C.M. and Vacca, J.P., *J. Med. Chem.*, 41 (1998) 3210. b. Sall, D.J., Bastian, J.A., Briggs, S.L., Buben, J.A., Chirgadze, N.I., Clawson, D.K., Denney, M.L., Giera, D.D., Gifford-Moore, D.S., Harper, R.W., Hauser, K.L., Klimkowski, V.J., Kohn, T.J., Lin, H., McCowan, J.R., Palkowitz, A.D., Smith, G.F., Takeuchi, K., Thrasher, K.J., Tinsley, J.M., Utterback, B.G., Yan, S.B. and Zhang, M., *J. Med. Chem.*, 40 (1997) 3489.
16. Priestle, J., Rahuel, J. and Gruetter, M., *Internal CIBA-Geigy Report* (11-06-93).